Journal of Clinical Immunology (2019) 39:776–785
https://doi.org/10.1007/s10875-019-00687-4

ORIGINAL ARTICLE

Novel Gain-of-Function Mutation in *Stat1* Sumoylation Site Leads to CMC/CID Phenotype Responsive to Ruxolitinib

Tariq Al Shehri[1,2] · Kimberly Gilmour[3] · Florian Gothe[1] · Sam Loughlin[4] · Shahnaz Bibi[4] · Andrew D. Rowan[1] · Angela Grainger[1] · Thivytra Mohanadas[1] · Andrew J. Cant[1,5] · Mary A. Slatter[1,5] · Sophie Hambleton[1,5] · Desa Lilic[1] · Timothy R. Leahy[6]

Received: 13 February 2019 / Accepted: 2 September 2019 / Published online: 11 September 2019

Abstract

Mutations in the coiled-coil and DNA-binding domains of *STAT1* lead to delayed STAT1 dephosphorylation and subsequently gain-of-function. The associated clinical phenotype is broad and can include chronic mucocutaneous candidiasis (CMC) and/or combined immunodeficiency (CID). We report a case of CMC/CID in a 10-year-old boy due to a novel mutation in the small ubiquitin molecule (SUMO) consensus site at the C-terminal region of *STAT1* leading to gain-of-function by impaired sumoylation. Immunodysregulatory features of disease improved after Janus kinase inhibitor (jakinib) treatment. Functional testing after treatment confirmed reversal of the STAT1 hyper-phosphorylation and downstream transcriptional activity. IL-17 and IL-22 production was, however, not restored with jakinib therapy (ruxolitinib), and the patient remained susceptible to opportunistic infection. In conclusion, a mutation in the SUMO consensus site of STAT1 can lead to gain-of-function that is reversible with jakinib treatment. However, full immunocompetence was not restored, suggesting that this treatment strategy might serve well as a bridge to definitive therapy such as hematopoietic stem cell transplant rather than a long-term treatment option.

Keywords STAT1 · sumoylation · combined immunodeficiency · chronic mucocutaneous candidiasis

Introduction

In 2011, heterozygous gain-of-function (GOF) mutations in the signal transducer and activator of transcription 1 (*STAT1*) gene were identified as the cause of autosomal dominant chronic mucocutaneous candidiasis (CMC) [1, 2]. The phenotype associated with GOF mutations in *STAT1* is now known to be broader than CMC and includes features of a combined immunodeficiency (CID) with autoimmunity, increased susceptibility to a broad range of pathogens, vascular aneurysms (both cerebral and extra-cerebral), aortic calcification, and an increased susceptibility to malignancy [3, 4]. These GOF mutations, for the most part, affect the coiled-coil (CCD) or DNA-binding domains (DBD) of *STAT1* [1–3, 5, 6]. Recent case reports also describe GOF-*STAT1* mutations in the SH2-domain [7–9], in the C-terminal domain [10], as well as in the linker domain of *STAT1* [11]. Hyper-phosphorylation of STAT1 due to delayed dephosphorylation in the nucleus has been documented as the molecular mechanism in most reported cases.

These mutations are GOF for STAT1-dependent cytokines such as interferon (IFN)-α, IFN-β, IFN-γ, and interleukin

Desa Lilic and Timothy R. Leahy contributed equally to this work.

Electronic supplementary material The online version of this article (https://doi.org/10.1007/s10875-019-00687-4) contains supplementary material, which is available to authorized users.

✉ Timothy R. Leahy
ronan.leahy@olchc.ie

[1] Institute of Cellular Medicine, Newcastle University, Newcastle upon Tyne, UK

[2] Present address: Department of Pathology & Laboratory Medicine, Immunology Lab, King Faisal Specialist Hospital & Research Centre, Riyadh, Kingdom of Saudi Arabia

[3] Department of Immunology, Camelia Botnar Laboratories, Great Ormond Street Hospital for Children, London, UK

[4] Regional Molecular Genetics Laboratory, Great Ormond Street Hospital for Children, London, UK

[5] Department of Paediatric Immunology and BMT, Great North Children's Hospital, Newcastle upon Tyne, UK

[6] Department of Paediatric Immunology and Infectious Diseases, Children's Health Ireland, Crumlin, Dublin D12 N512, Ireland

(IL)-27. They lead to increased expression of STAT1-dependent genes and decreased expression of STAT3-dependent genes [12]. Patients with STAT1-GOF mutations demonstrate reduced or absent IL-17 and IL-22 production and reduced proportions of IL-17 and IL-22-producing T-cells. This explains, in part at least, their increased susceptibility to mucosal candidiasis and infections with extracellular bacteria.

Small ubiquitin-related modifier (SUMO) is an 11-kDa ubiquitin-like protein that, once bound, tags proteins for degradation. STAT1 is subject to post-translational reversible modification through conjugation with SUMO, a process known as sumoylation. Sumoylation can affect the biological activity of the target protein including signal transduction and transcriptional activation. SUMO conjugation on STAT1 occurs on a single lysine residue at position 703 within the SUMO consensus motif ($702_{IKTE}705$) at the C-terminal region of the protein. Several studies suggest that sumoylation has a negative regulatory effect on STAT1-induced gene responses, including the cellular response to IFN-γ [13–15].

A recently published case report described a patient with CID associated with a mutation (E705V) in the SUMO consensus motif of STAT1 [10]. The mutation led to the disruption of sumoylation which increased transcriptional activity, thereby demonstrating a new mechanism for GOF in STAT1-related disease. Clinical disease associated with GOF mutations in *STAT1* has been treated with at least partial success by the use of Janus kinase inhibitors (jakinibs) such as ruxolitinib which block the effect of STAT-mediated cytokines [16, 17].

We report a second case of CMC and CID associated with a GOF mutation (E705Q) in the SUMO consensus site of STAT1. We describe the clinical and immunological characteristics as well as the impact of ruxolitinib therapy on our patient, specifically on cytokine-stimulated STAT1/STAT3 phosphorylation, STAT1/STAT3-dependent gene expression, IL-17/IL-22 cytokine production, and STAT1 dephosphorylation kinetics, as well as the clinical features.

Methods

STAT1 Sequencing

DNA extracted from peripheral blood was screened for variants in 72 genes involved in primary immune deficiencies using the Agilent QXT Target Enrichment system according to the manufacturer's protocol (Version B.2, October 2014) for Illumina sequencing. Briefly, genomic DNA was sonically sheared to 300 bp on the Covaris S2 system (Covaris, MA, USA) and ligated with SureSelect Adaptor Oligo Mix. The fragment size was assessed using the TapeStation 2100 Bioanalyzer (Agilent Technologies). The adaptor-ligated libraries were then amplified and hybridized to our customized SureSelect panel. Captured libraries were index barcoded, pooled, and sequenced as multiplex of 16 samples on an Illumina MiSeq sequencer in 150 bp paired-end mode according to the standard protocol for this platform. Analysis of data in Fastq format from the MiSeq sequencing instrument was subject to genome-wide alignment (BWA-mem) (Hg19), variant calling (Freebayes), and variant annotation (Alamut-batch) using an in-house pipeline, developed at the NE Thames Regional Genetics laboratory, which has been validated and shown to be 97.5% sensitive (95% confidence interval) for single-base substitutions and small insertion/deletion variants in regions covered by 30 or more reads.

Sequence variants were filtered by the in-house pipeline; variants had to be present in 20% of at least 30 reads to be called. Filtering removed variants present at 2% or greater in Exome Variant Server, or EVS (http://evs.gs.washington.edu/EVS), or 1000 genomes datasets (http://www.internationalgenome.org), or in > 3 patients on a run of 16, unless detected in patients with the same clinical diagnosis. Filtered variants were checked against relevant databases, such as HGMD (http://www.hgmd.cf.ac.uk/ac/index.php), local databases, and Clinvar (https://www.ncbi.nlm.nih.gov/clinvar/) to assess for previous publication. Pathogenicity was assessed using Polyphen2 (http://genetics.bwh.harvard.edu/pph2/), Align GVGD (http://agvgd.hci.utah.edu/), and Mutation Taster (http://mutationtaster.org/) prediction algorithms.

Primers for variant confirmation were designed using Primer 3 software (http://bioinfo.ut.ee/primer3). The *STAT1* variant identified was described according to HGVS guidelines (http://www.hgvs.org/) relative to reference sequence NM_007315.3, where nucleotide number 1 corresponds to the A of the ATG translation initiation codon.

Blood Samples and Cell Lines

Following written informed consent, heparinized blood samples were taken from a patient and a healthy "travel" control, and processed in an identical manner. Patient samples were collected before commencing treatment with ruxolitinib and again 6 months into therapy. Functional assays were conducted on whole blood or peripheral blood mononuclear cells (PBMCs) and Epstein-Barr virus (EBV)-transformed B cell lines from healthy controls and CMC patients with confirmed GOF-STAT1 mutations following informed written consent, isolated and cultured as previously described [12]. Ethical approval was granted by the Great North Biobank (GNB), Reference No. 5458/10/H0906/22, and Newcastle Autoimmune Inflammatory Rheumatic Diseases (NAIRD) Research Biobank, Reference No. 10/H0106/30.

Evaluation of STAT1 and STAT3 Phosphorylation by Flow Cytometry

Tyrosine 701 (Tyr701) STAT1 phosphorylation (pSTAT1) and Tyr705 STAT3 phosphorylation (pSTAT3) were assessed in

whole blood or EBV-derived B cell lines stimulated with IFN-α 1000 IU/ml (IntronA/IFN-α2b, MSD), IFN-γ 1 μg/ml, or IL-6 0.1 μg/ml IL-6 (both from R&D Systems) for 15 or 30 min at 37 °C. Cells were fixed with Lyse/Fix buffer, permeabilized with Phosflow Perm buffer III, and stained for pSTAT1 (Alexa Fluor 647) and pSTAT3 (Alexa Fluor 488; Becton Dickinson, UK). Surface staining was performed using CD3 (BV421, Biolegend, UK). Data were collected with a FACSCanto II (BD Biosystems, UK) and analyzed with the FlowJo software (BD Biosystems). STAT1 and STAT3 phosphorylation was also assessed in EBV-transformed B cell lines, stimulated with cytokines as above. pSTAT1, total STAT1 (clone 1/STAT1), pSTAT3, and appropriate isotype controls (antibodies all from BD) were stained in a separate unstimulated sample. Cells surface staining of B cells was performed using CD19+ antibody (Biolegend, UK). A detailed description of the methodology used for this experiment is included in the supplementary data.

Evaluation of STAT1 and STAT3 Phosphorylation Using Western Blotting

Altered STAT1 and STAT3 phosphorylation by flow cytometry was confirmed with western blotting (WB) as the gold-standard method. Isolated PBMCs were stimulated for 30 min with IFN-α 1000 IU/ml or IFN-γ 1 μg/ml or left unstimulated. Cells were lysed in buffer (CellLytic M, Sigma) containing Phosphatase Inhibitor Cocktail (Thermo Scientific) and Protease Inhibitor Cocktail Tablet (Roche). Equi-protein lysates were transferred to PVDF membranes (Millipore) and incubated with primary antibodies to STAT1, pSTAT1, STAT3, pSTAT3, or GAPDH (all from Cell Signalling) followed by HRP-conjugated goat anti-rabbit antibody (Dako). Blots were developed and visualized by enhanced chemiluminescence using the Immobilon Western detection system (Millipore) and Amersham ECL detection reagents (GE Healthcare) according to the manufacturer's instructions. Evaluation of total STAT1 concentration by WB was undertaken in EBV-transformed B cells from the patient, healthy controls, and disease controls (CMC patients with GOF-STAT1 mutations A267V and R274W). A detailed description of the methodology used for this experiment is included in the supplementary data.

Evaluation of STAT1- and STAT3-Related Transcriptional Activity

The effect of the E705Q *STAT1* mutation on STAT1- and STAT3-dependent gene transcription was assessed by mRNA expression using quantitative reverse transcriptase PCR (qRT-PCR) in PBMCs and EBV cell lines from both the patient and healthy control. CXCL9, CXCL10, and IRF1 (STAT1-dependent genes) as well as cFos and cMyc (STAT3-dependent genes) mRNA expression was assessed in cells stimulated with IFN-α 1000 IU/ml or IFN-γ 1 μg/ml for 4 h in qRT-PCR TaqMan expression assays, using the ABI Prism 7900HT sequence detection system for PCR cycling and detection (Applied Biosystems). 18S rRNA was used as a normalization control.

Evaluation of Cytokine Production

In order to investigate IL-17 and IL-22 cytokine levels ex vivo as well as following in vitro stimulation, we assessed production both in whole blood and PBMCs after mitogen or antigen stimulation.

Ex vivo cytokine production was assessed in heparinized, diluted (1:5) whole blood stimulated with 10 μg/ml of mitogen phytohemagglutinin (PHA, Sigma) or left unstimulated for 1 day in a 37 °C, 5% CO_2 incubator.

For In vitro cytokine production, PBMCs (3×10^6/ml) were cultured for 5 days in tissue culture medium (TCM) (RPMI-1640, 2 mM L-glutamine, 100 IU/ml penicillin, 100 μg/ml streptomycin (all from Sigma, UK)) supplemented with 10% fetal calf serum (FCS, Lonza, Cambridge, UK), stimulated with live *Candida albicans* (1:15,000, ATCC, USA) or 5 μg/ml PHA with addition of 2.5 μg/ml Amphotericin B (Sigma) to prevent *Candida* overgrowth, or left unstimulated in a 37 °C, 5% CO_2 incubator.

Cytokine levels in culture supernatants were assessed by IL-17A and IL-22 Ready-Set-Go ELISA kits (eBioscience, USA) according to manufacturer's instructions. The ELISA sensitivity cut-off to IL-17/IL-22 levels was 0.5 pg/ml.

Evaluation of pSTAT1 Dephosphorylation Kinetics

The dephosphorylation kinetic rate of pSTAT1 was assessed in EBV-transformed B cell lines from the patient, a healthy control, and a disease control (STAT1 GOF mutation A267V). Cells were stimulated with IFN-α 1000 IU/ml for 30 min. pSTAT1 expression was analyzed at 30 min, 1 h, 2 h, 3 h, 4 h, 5 h, and 6 h by flow cytometry as described above.

Statistical Analysis

Statistical analysis and plotting of data were performed using the GraphPad Prism Version 7.0 software (San Diego, CA, USA). Unpaired Student's *t* test was used to compare the expression of STAT1- and STAT3-stimulated genes between the patient and the healthy control in qPCR experiments ($P < 0.05$).

Results

Clinical Case Description

Clinical Features

The patient was a 10-year-old boy of Irish Caucasian descent with no known family history of autoimmunity or immunodeficiency. He initially presented to the immunology clinic at 4 years of age with a history of recurrent respiratory tract infections from the age of 6 months that continued throughout early childhood. He previously underwent placement of myringotomy tubes for recurrent otitis media and bronchoscopy for chronic unremitting cough. Bronchoalveolar lavage was positive for both *Streptococcus pneumoniae* and *Haemophilus influenzae* by culture. The patient had a history of chronic mucocutaneous candidiasis (CMC) with both oral candidiasis and a granulomatous folliculitis. The patient subsequently demonstrated increased susceptibility to viral infections. Specifically, he had a history of severe varicella and recurrent herpes zoster. He developed chronic severe molluscum contagiosum on his thighs and buttocks that persisted for 3 years, and ultimately resolved only after a prolonged treatment course of topical cidofovir.

In addition to his increased susceptibility to infection, the patient suffered from severe recurrent aphthous stomatitis that did not respond to topical corticosteroid therapy. The patient also demonstrated lymphoproliferation, with splenomegaly and lymphadenopathy appreciable both on clinical examination and on imaging. Results of lymphocyte immunophenotyping showed significant CD4 T cell lymphopenia, and measurement of serum immunoglobulins demonstrated undetectable IgG2 (before replacement therapy) as described (Table S1). T cell proliferation assays were normal, as was the T cell TCR-vβ repertoire.

Genetic Testing

A heterozygous missense variant c.2113G>C p.(Glu705Gln, E705Q) was identified in the *STAT1* gene using next-generation sequencing (Figure S1) and confirmed by the Sanger sequencing according to standard methods (Fig. 1). This mutation affected a highly conserved amino acid within the SUMO consensus site ($702_{IKTE}705$) in the C-terminal region and was predicted to abolish STAT1 sumoylation [18]. Sequencing of the *AIRE* gene demonstrated no pathogenic mutations. To date, the patient's immediate family members (all asymptomatic) have not been screened for the STAT1 variant, precluding any comment on expressivity, penetrance, or inheritance.

Management

The patient's susceptibility to infection improved with antimicrobial prophylaxis (including azithromycin, fluconazole, and valaciclovir) and immunoglobulin replacement therapy, but he continued to have severely disabling symptoms associated with recurrent severe aphthous stomatitis and generalized

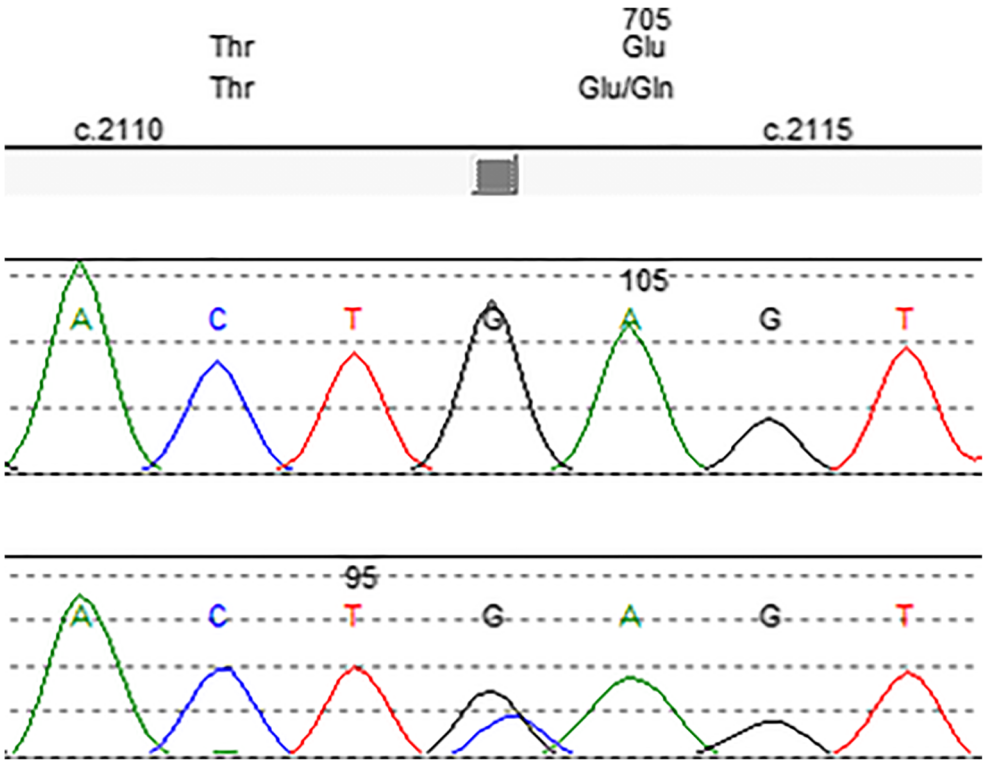

Fig. 1 E705Q mutation in STAT1 confirmed by the Sanger sequencing

fatigue. These symptoms improved significantly shortly after commencing a trial of the JAK1/2 Janus kinase inhibitor (ruxolitinib) at a dose of 25 mg twice daily (33 mg/m^2/day). Of note, fluconazole prophylaxis had been discontinued at this point and the dose of ruxolitinib was adjusted downwards by 50% when fluconazole was later re-commenced. However, the patient suffered a number of significant infections while receiving ruxolitinib including an episode of herpes zoster and a lower respiratory tract infection requiring hospitalization and IV antibiotic therapy. A decision was made to proceed to hematopoietic stem cell transplantation (HSCT). He subsequently underwent a successful matched unrelated donor HSCT (conditioned with alemtuzumab, treosulfan, fludarabine, plerixafor, and gCSF) and graft-versus-host disease (GvHD) prophylaxis with cyclosporine and mycophenolate mofetil. HSCT was complicated by grade 2 skin GvHD and disseminated adenoviral infection, but the patient has made a full recovery and is now symptom-free 15 months post-HSCT with 100% donor myeloid and donor B cell chimerism and 81% donor T cell chimerism.

Functional Immunology Testing

STAT1 and STAT3 Phosphorylation Assays

Flow Cytometry

We demonstrated hyper-phosphorylation of pSTAT1 as measured by increased levels of intracellular pSTAT1 in whole blood CD3+ T lymphocytes (Fig. 2a) as well as in CD19+ EBV-transformed B cells (not shown) after stimulation with cytokines in patient's cells in comparison with the healthy control. Repeat measurements taken after the patient had received ruxolitinib therapy (Fig. 2b) demonstrated that the hyper-phosphorylation had been reduced to control levels.

Western Blotting

Increased pSTAT1 in the patient's cells was confirmed by western blotting in whole cell lysates of PBMC from the patient and healthy control (Fig. 3). Before ruxolitinib treatment

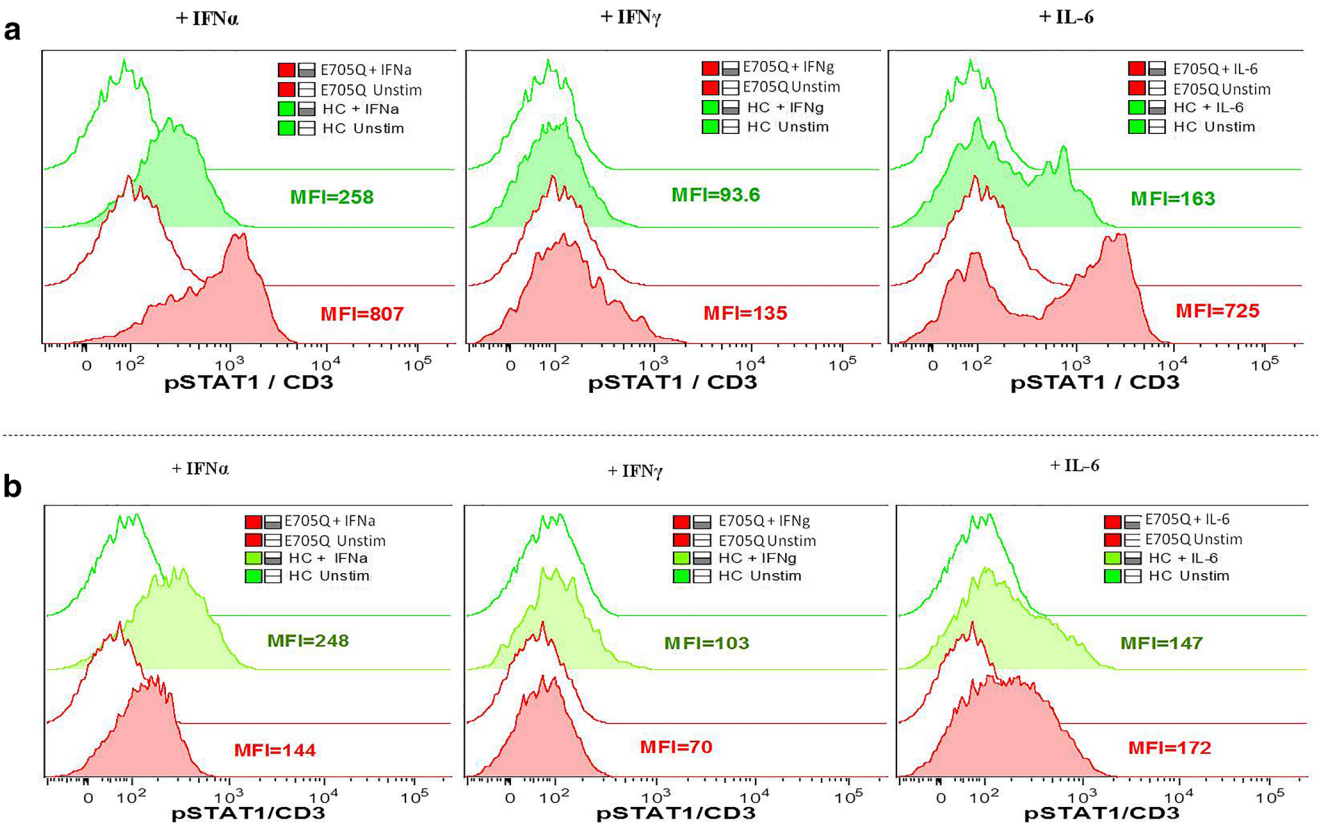

Fig. 2 Ruxolitinib in vivo reverses hyper-phosphorylation of STAT1 in T cells from the patient (E705Q) as assessed by intracellular flow cytometry. Flow cytometry on whole blood from the patient (E705Q, red) and a healthy control (HC, green) before (**a**) and 6 months after commencing ruxolitinib therapy (**b**). Cells were stimulated for 15 min with IFN-α (1000 IU/ml), IFN-γ (1 μg/ml), and IL-6 (0.1 μg/ml) or left unstimulated (unstim). Flow cytometry was performed with cell-surface staining (CD3) and intracellular staining (pSTAT1). Filled histograms represent stimulated samples. Numbers indicate the median fluorescence intensity (MFI) of phosphorylation. Data were gated and analyzed using the FlowJo software. Hyper-phosphorylation of STAT1 in T cells in response to cytokine stimulation normalized after ruxolitinib therapy

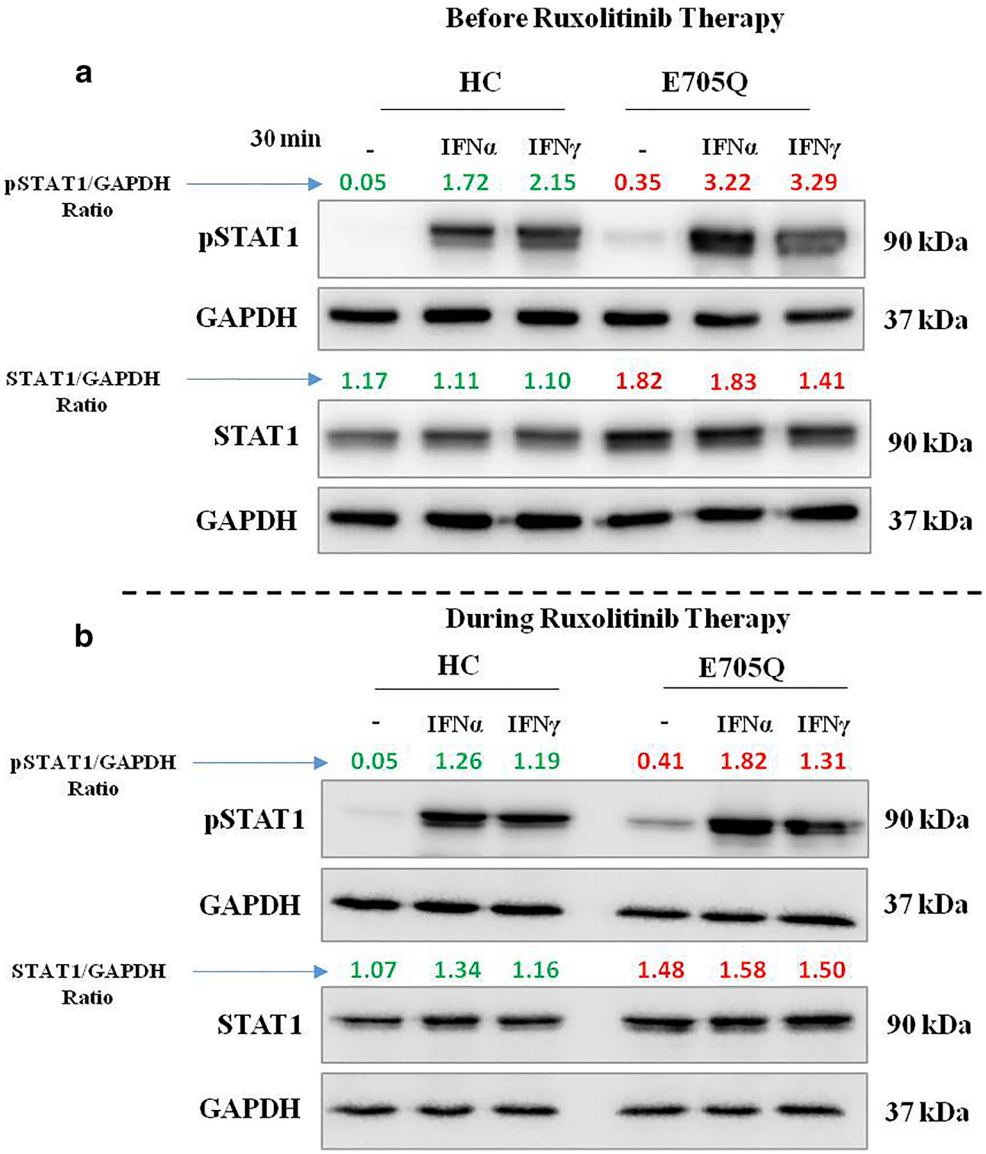

Fig. 3 pSTAT1 protein levels as measured by western blotting in PBMC lysates from the patient (E705Q) are elevated in comparison to healthy control (HC) at baseline (**a**) and normalized after ruxolitinib therapy (**b**). Cells were left unstimulated (−) or stimulated with IFN-α (1,000 IU/ml) or IFN-γ (1 μg/ml) for 30 min. The relative intensity of the blots (shown above bands) was corrected for the background and normalized to GADPH (control). Band intensity was analyzed using ImageJ software. Treatment with ruxolitinib normalizes pSTAT1 protein levels in the patient's PBMC as evident from the reduction in band intensity after both IFN-α and IFN-γ stimulation

(Fig. 3a), in unstimulated conditions, pSTAT1, as measured by the ratio of the phosphorylated band to the loading control (GADPH), was undetectable in the control sample and only barely visible in the patient. However, after stimulation with IFNs, pSTAT1 was significantly increased in patient cells. Repeat measurements undertaken while the patient was on ruxolitinib treatment (Fig. 3b) demonstrated that pSTAT1 levels in patient cells were significantly decreased and were now similar to control levels. Levels of STAT3 and pSTAT3 did not differ appreciably between the patient and the healthy control (Figure S2).

STAT1- and STAT3-Related Transcriptional Activity

The transcriptional activation of STAT1-dependent genes (CXCL9, CXCL10, and IRF1) in the patient's cells before ruxolitinib treatment was markedly enhanced compared with those in healthy control (Fig. 4a). This increased transcriptional activity was attenuated by treatment with ruxolitinib (Fig. 4b). Transcriptional activation of STAT3-dependent genes (cFos and cMyc) in the patient's cells before treatment was decreased compared with those in a healthy control (Figure S3).

IL-17 and IL-22 Production

In ex vivo 1-day whole blood cultures, IL-17 was not measurable in supernatant from unstimulated cells collected from either the patient or a healthy control; in PHA-stimulated whole blood, IL-17 was measurable in the healthy control supernatant but not in patient supernatant (Figure S4, Table S2). These results were not altered by ruxolitinib therapy. IL-22 was not produced in either patient or control in these conditions.

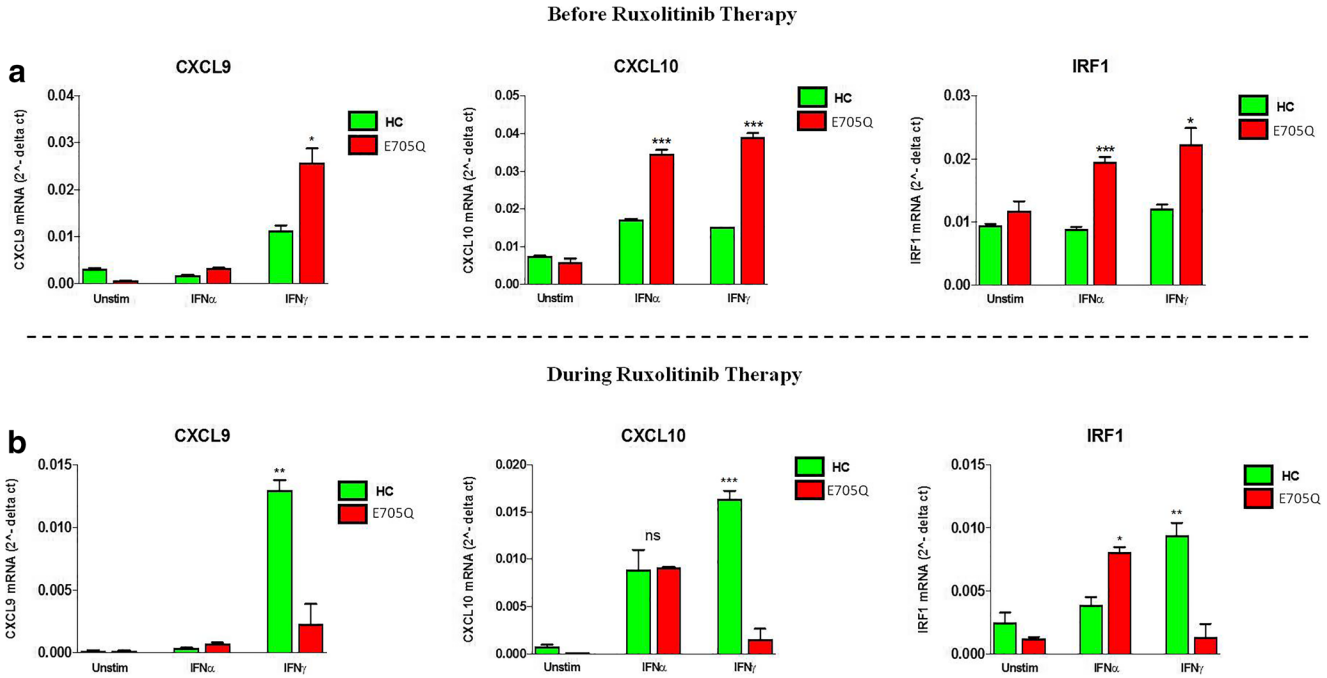

Fig. 4 Expression of STAT1-dependent genes (CXCL9, CXCL10, IRF8) increased in PBMC from the patient (E705Q) in comparison with healthy control (HC) at baseline (**a**) and reversed after 6 months of ruxolitinib therapy (**b**). Cells were left unstimulated (unstim) or stimulated with IFN-α (1000 IU/ml) or IFN-γ (1 μg/ml) for 4 h. The data were analyzed using 18S rRNA as a reference gene. *P* value was calculated using the unpaired *t* test (*$P < 0.05$, **$P < 0.01$, *** $P < 0.001$; NS, not statistically significant). The expression of STAT1-dependent genes in PBMC from E705Q at baseline (**a**) was significantly elevated in comparison with the HC. This difference was eliminated (and in some cases reversed) after 6 months of treatment with ruxolitinib

Ex vivo 5-day PBMCs cultures demonstrated detectable IL-17 production after stimulation with both PHA and *C. albicans* in the cell supernatants of control samples but not in the patient (Fig. 5a). Treatment with ruxolitinib did not restore either IL-17 or IL-22 production in the patient (Fig. 5b, Table S3). Under similar culture conditions, IL-22 was detectable after stimulation with both PHA and *C. albicans* in cell supernatants from the healthy control but not from the patient (Figure S5, Table S4).

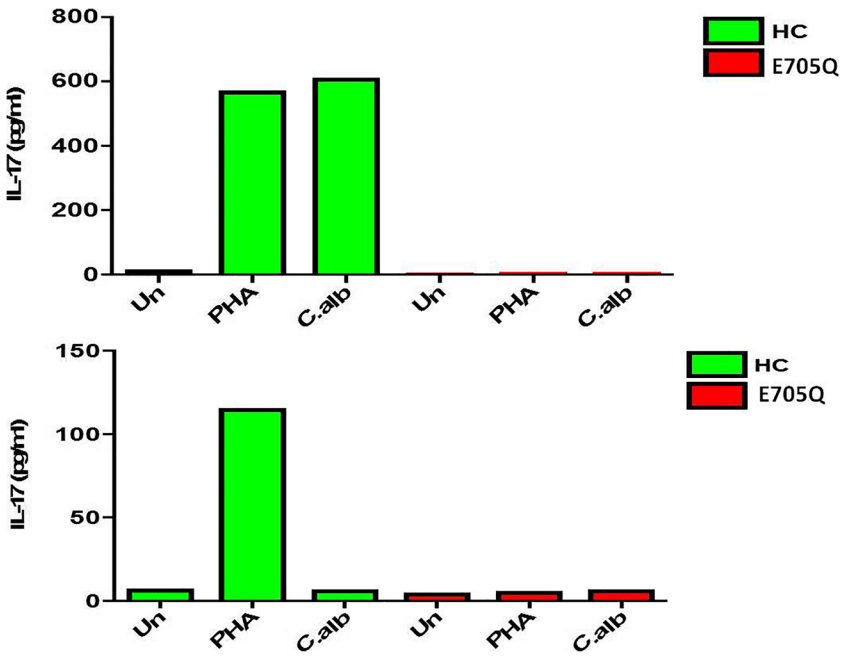

Fig. 5 PBMC IL-17 production as measured by ELISA in the patient before and after ruxolitinib therapy. Cytokine production of IL-17 in unstimulated, PHA (5 μg/ml)-stimulated and *C. albicans* (1:15,000)-stimulated PBMC was assessed in the patient (E705Q) and a healthy control (HC) at baseline (**a**) and after treatment with ruxolitinib (**b**). PBMC culture supernatants were harvested after 5 days and the level of IL-17 was measured with ELISA. Treatment with ruxolitinib did not restore PBMC IL-17 production in our patient

Dephosphorylation Assay

The rate of pSTAT1 dephosphorylation in the patient was similar to that seen in a healthy control (Fig. 6). Delayed dephosphorylation was seen in cells from an unrelated GOF-STAT1 patient with a classical CCD (A267V) mutation (Fig. 6). Results from both flow cytometry and WB (supplementary Figure S6 and S7) did not demonstrate a statistically significant difference in tSTAT1 between healthy controls, our patient, and GOF-STAT1 disease controls with heterozygous classical CCD mutations A267V and R274W.

Discussion

This case is the second published description of a patient with CID related to a GOF mutation in the SUMO consensus site of STAT1. In common with the previous case described by Sampaio et al. [10], we confirmed increased STAT1 activity, i.e., STAT1 gain-of-function by both an increase in pSTAT1 expression in our patient along with increased transcriptional activity in STAT1-dependent genes. Using a dephosphorylation assay, we were able to demonstrate that, unlike the disease control (STAT1-GOF mutation A267V in the CCD), GOF in this instance was likely due to impaired sumoylation rather than impaired dephosphorylation only. Delayed dephosphorylation has been reported in GOF-STAT1 patients before and attributed to impaired binding of phosphatases to mutant STAT1, thereby impairing dephosphorylation [1, 19–21].

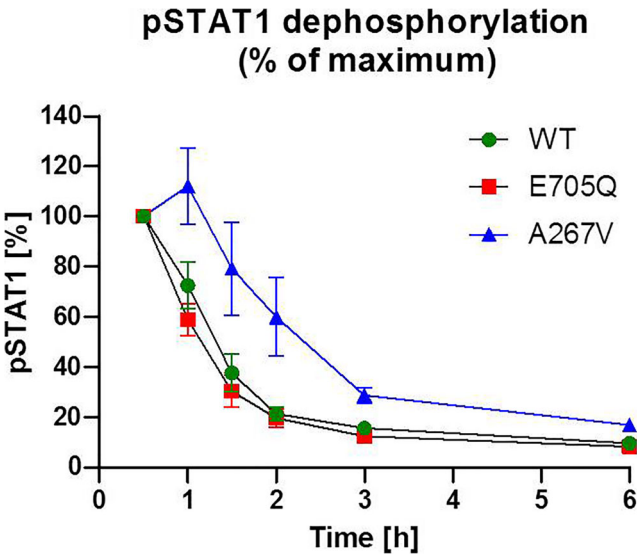

Fig. 6 Dephosphorylation kinetics of pSTAT1 in EBV-B cells from the patient (E705Q) compared with the disease control (GOF-STAT1 A267V mutation) and healthy (wild type, WT) control. After stimulation with IFN-α (1000 IU/ml), at the indicated times, cells were fixed and permeabilized for cell-surface staining (CD19) and intracellular staining (pSTAt1) and measured by flow cytometry. To follow dephosphorylation kinetics, MFIs within individual time courses are related to the 30-min time point (assumed maximum phosphorylation) and expressed as percentages. Medians of at least 3 replicates per sample are shown

Alternatively, delayed dephosphorylation might also occur if baseline total STAT1 levels are elevated, resulting in the generation of more pSTAT1 that takes longer to dephosphorylate. Such a mechanism has been reported by several laboratories in patients with classical GOF-STAT1 mutations, who in addition document increased rather than impaired dephosphorylation in this context [22, 23]. Our own results do not confirm these findings. We did however note substantial variability in total STAT1 protein levels including in healthy controls. The reason for this obvious discrepancy in numerous reports remains to be clarified.

We were also able to demonstrate that ruxolitinib therapy attenuated the increase in both phosphorylation of E705Q-mutant STAT1 and its downstream increased transcriptional activity. This coincided with an improvement in symptoms associated with the immunodysregulatory features of STAT1-GOF disease (in this case fatigue and severe aphthous stomatitis) and mirrors the previous experience of the use of ruxolitinib in STAT1-GOF [16, 17].

Treatment with ruxolitinib did not restore IL-17 or IL-22 production in either whole blood or PBMC isolated from the affected patient. This failure to restore IL-17 production has been described previously [24, 25]. Failure to restore IL-17 production may be related to persistent inhibition of STAT3 function, since STAT3 is critical for differentiation of T_H17 cells, mediating the signalling of T_H17-inducing cytokines such as IL-6, IL-10, and IL-21 [26]. Impaired restoration of IL-17 might account for ongoing increased susceptibility to infection in the patient, as manifest by a radiologically proven lower respiratory tract infection and an episode of herpes zoster occurring on ruxolitinib therapy, both infections are known manifestations of STAT3 loss of function [27]. Zimmerman et al. demonstrated a dose-dependent inhibitory effect of ruxolitinib on IL-17 production, suggesting that the mechanism may be a direct effect of the drug rather than a failure to re-balance STAT1/STAT3 signalling [24]. Since ruxolitinib is both a JAK1/JAK2 inhibitor, impaired STAT3 signalling on ruxolitinib may result from inhibition of T_H17 differentiation from naive T cells mediated by IL-6 and IL-23 via JAK2:TYK2 [26, 28]. Upadacitinib, a selective JAK1 inhibitor, has recently become available and shows promise as a second-line treatment in rheumatoid arthritis [29]. This may be a better choice for treatment of STAT1-GOF-related clinical features (in particular autoinflammatory and autoimmune) since it might potentially avoid/reduce this inhibition of STAT3 signalling [30]. However, this reasoning may be overly simplistic. A recent case series by Kaleviste et al. demonstrated evidence of epigenetically determined changes in interferon-stimulated gene expression in patients with STAT1-GOF disease that might explain the limited effect of JAK1/2 inhibition in such patients [31]. A therapeutic

approach that targets epigenetic gene expression such as histone deacetylation inhibition might be promising in this context [32].

As it stands, patients with GOF-STAT1 mutations who do not meet criteria for HSCT may require prolonged treatment with jakinibs. Further information on the long-term effects of jakinibs, in particular infection risk, is needed to inform our decision-making in such instances.

To conclude, mutations in *STAT1* that affect sumoylation consensus site can lead to gain-of-function. Jakinibs can ameliorate immunodysregulatory features associated with STAT1 GOF in such cases but do not appear to restore immune competence completely. Jakinibs might serve well as a bridge to definitive therapy rather than a long-term treatment strategy, particularly JAK1-selective inhibitors once they become more widely available.

Acknowledgments The authors wish to acknowledge the good will of the patient and his parents for consenting to publication of this case report.

Author Contributions TAS, ADR, DL: functional immunology laboratory experiments, manuscript preparation, and review.

SL, SB: NGS panel and Sanger sequencing of *STAT1* gene, manuscript preparation, and review.

KG, AJC, MAS, TRL: manuscript preparation and review.

Funding Information Authors DL and TAS were funded to undertake this research through a Medical Research Council Confidence in Concept Grant (Grant No. BH152850). Author TAS was funded by King Faisal Specialist Hospital & Research Centre grant, Saudi Arabia. Author FG was funded by Deutsche Forschungsgemeinschaft (GO2955/1-1 (F.G.)).

Compliance with Ethical Standards

Ethical approval was granted by the Great North Biobank (GNB), Reference No. 5458/10/H0906/22, and Newcastle Autoimmune Inflammatory Rheumatic Diseases (NAIRD) Research Biobank, Reference No. 10/H0106/30.

Conflict of Interest The authors declare that they have no conflict of interest.

References

1. Liu L, Okada S, Kong XF, Kreins AY, Cypowyj S, Abhyankar A, et al. Gain-of-function human STAT1 mutations impair IL-17 immunity and underlie chronic mucocutaneous candidiasis. J Exp Med. 2011;208(8):1635–48.
2. van de Veerdonk FL, Plantinga TS, Hoischen A, Smeekens SP, Joosten LAB, Gilissen C, et al. STAT1 mutations in autosomal dominant chronic mucocutaneous candidiasis. N Engl J Med. 2011;365(1):54–61.
3. Toubiana J, Okada S, Hiller J, Oleastro M, Lagos Gomez M, Aldave Becerra JC, et al. Heterozygous STAT1 gain-of-function mutations underlie an unexpectedly broad clinical phenotype. Blood. 2016;127(25):3154–64.
4. Smyth AE, Kaleviste E, Snow A, Kisand K, McMahon CJ, Cant AJ, et al. Aortic calcification in a patient with a gain-of-function STAT1 mutation. J Clin Immunol. 2018;38(4):468–70.
5. Takezaki S, Yamada M, Kato M, Park MJ, Maruyama K, Yamazaki Y, et al. Chronic mucocutaneous candidiasis caused by a gain-of-function mutation in the STAT1 DNA-binding domain. J Immunol. 2012;189(3):1521–6.
6. Depner M, Fuchs S, Raabe J, Frede N, Glocker C, Doffinger R, et al. The extended clinical phenotype of 26 patients with chronic mucocutaneous candidiasis due to gain-of-function mutations in STAT1. J Clin Immunol. 2016;36:73–84.
7. Meesilpavikkai K, Dik WA, Schrijver B, et al. A novel heterozygous mutation in the STAT1 SH2 domain causes chronic mucocutaneous candidiasis, atypically diverse infections, autoimmunity, and impaired cytokine regulation. Front Immunol. 2017;8:274.
8. Al Dhanhani H, Al Shehri T, Lilic D, et al. Double trouble? CMC with a mutation in both AIRE and STAT1. J Clin Immunol. 2018;38(6):635–7.
9. Sobh A, Chou J, Schneider L, Geha RS, Massaad MJ. Chronic mucocutaneous candidiasis associated with an SH2 domain gain-of-function mutation that enhances STAT1 phosphorylation. J Allergy Clin Immunol. 2016;138(1):297–9.
10. Sampaio EP, Ding L, Rose SR, Cruz P, Hsu AP, Kashyap A, et al. Novel signal transducer and activator of transcription 1 mutation disrupts small ubiquitin-related modifier conjugation causing gain of function. J Allergy Clin Immunol. 2018;141(5):1844–1853 e1842.
11. Weinacht KG, Charbonnier LM, Alroqi F, Plant A, Qiao Q, Wu H, et al. Ruxolitinib reverses dysregulated T helper cell responses and controls autoimmunity caused by a novel signal transducer and activator of transcription 1 (STAT1) gain-of-function mutation. J Allergy Clin Immunol. 2017;139(5):1629–1640 e1622.
12. Zheng J, van de Veerdonk FL, Crossland KL, Smeekens SP, Chan CM, al Shehri T, et al. Gain-of-function STAT1 mutations impair STAT3 activity in patients with chronic mucocutaneous candidiasis (CMC). Eur J Immunol. 2015;45(10):2834–46.
13. Ungureanu D, Vanhatupa S, Kotaja N, et al. PIAS proteins promote SUMO-1 conjugation to STAT1. Blood. 2003;102(9):3311–3.
14. Ungureanu D, Vanhatupa S, Gronholm J, et al. SUMO-1 conjugation selectively modulates STAT1-mediated gene responses. Blood. 2005;106(1):224–6.
15. Begitt A, Droescher M, Knobeloch KP, Vinkemeier U. SUMO conjugation of STAT1 protects cells from hyperresponsiveness to IFNgamma. Blood. 2011;118(4):1002–7.
16. Higgins E, Al Shehri T, McAleer MA, et al. Use of ruxolitinib to successfully treat chronic mucocutaneous candidiasis caused by gain-of-function signal transducer and activator of transcription 1 (STAT1) mutation. J Allergy Clin Immunol. 2015;135(2):551–3.
17. Forbes LR, Vogel TP, Cooper MA, Castro-Wagner J, Schussler E, Weinacht KG, et al. Jakinibs for the treatment of immune dysregulation in patients with gain-of-function signal transducer and activator of transcription 1 (STAT1) or STAT3 mutations. J Allergy Clin Immunol. 2018;142(5):1665–9.
18. Gronholm J, Vanhatupa S, Ungureanu D, et al. Structure-function analysis indicates that sumoylation modulates DNA-binding activity of STAT1. BMC Biochem. 2012;13:20.
19. Sampaio EP, Hsu AP, Pechacek J, Bax HI, Dias DL, Paulson ML, et al. Signal transducer and activator of transcription 1 (STAT1) gain-of-function mutations and disseminated coccidioidomycosis and histoplasmosis. J Allergy Clin Immunol. 2013;131(6):1624–34.
20. Uzel G, Sampaio EP, Lawrence MG, Hsu AP, Hackett M, Dorsey MJ, et al. Dominant gain-of-function STAT1 mutations in FOXP3 wild-type immune dysregulation-polyendocrinopathy-enteropathy-X-linked-like syndrome. J Allergy Clin Immunol. 2013;131(6):1611–23.

21. Mizoguchi Y, Tsumura M, Okada S, Hirata O, Minegishi S, Imai K, et al. Simple diagnosis of STAT1 gain-of-function alleles in patients with chronic mucocutaneous candidiasis. J Leukoc Biol. 2014;95(4):667–76.
22. Bernasconi AR, Yancoski J, Villa M, Oleastro MM, Galicchio M, Rossi JG. Increased STAT1 amounts correlate with the phospho-STAT1 level in STAT1 gain-of-function defects. J Clin Immunol. 2018;38(7):745–7.
23. Zimmerman O, Olbrich P, Freeman AF, Rosen LB, Uzel G, Zerbe CS, et al. STAT1 gain-of-function mutations cause high total STAT1 levels with normal dephosphorylation. Front Immunol. 2019;10:1433.
24. Zimmerman O, Rosler B, Zerbe CS, et al. Risks of ruxolitinib in STAT1 gain-of-function-associated severe fungal disease. Open Forum Infect Dis. 2017;4(4):ofx202.
25. Bloomfield M, Kanderova V, Parackova Z, et al. Utility of ruxolitinib in a child with chronic mucocutaneous candidiasis caused by a novel STAT1 gain-of-function mutation. J Clin Immunol. 2018;38:589–601.
26. Mogensen TH. IRF and STAT transcription factors - from basic biology to roles in infection, protective immunity, and primary immunodeficiencies. Front Immunol. 2019;9:3047.
27. Siegel AM, Heimall J, Freeman AF, Hsu AP, Brittain E, Brenchley JM, et al. A critical role for STAT3 transcription factor signaling in the development and maintenance of human T cell memory. Immunity. 2011;35(5):806–18.
28. Virtanen AT, Haikarainen T, Raivola J, et al. Selective JAKinibs: prospects in inflammatory and autoimmune diseases. BioDrugs. 2019;33(1):15–32.
29. Serhal L, Edwards CJ. Upadacitinib for the treatment of rheumatoid arthritis. Expert Rev Clin Immunol. 2018:1–13.
30. Al Shehri T, Abinun M, Gennery AR, et al. Is gain-of-function STAT1 CMC an interferonopathy? Clin Exp Immunol. 2015;182(S1):15.
31. Kaleviste E, Saare M, Leahy TR, Bondet V, Duffy D, Mogensen TH, et al. Interferon signature in patients with STAT1 gain-of-function mutation is epigenetically determined. Eur J Immunol. 2019;49(5):790–800.
32. van de Veerdonk FL, Netea MG. Treatment options for chronic mucocutaneous candidiasis. J Inf Secur 2016:72 Suppl:S56–S60.